Published in final edited form as:
Water Resour Res. 2016 July ; 52(7): 5393–5399. doi:10.1002/2016WR018775.

Comparison of Fluid-Fluid Interfacial Areas Measured with X-ray Microtomography and Interfacial Partitioning Tracer Tests for the same Samples

Kieran McDonald[1], **Kenneth C. Carroll**[2], and **Mark L. Brusseau**[1,3,*]

[1]Soil, Water, and Environmental Science Dept., University of Arizona

[2]Dept. of Plant & Environmental Sciences, New Mexico State University

[3]Hydrology and Water Resources Dept., University of Arizona

Abstract

Two different methods are currently used for measuring interfacial areas between immiscible fluids within 3-D porous media, high-resolution microtomographic imaging and interfacial partitioning tracer tests (IPTT). Both methods were used in this study to measure non-wetting/wetting interfacial areas for a natural sand. The microtomographic imaging was conducted on the same packed columns that were used for the IPTTs. This is in contrast to prior studies comparing the two methods, for which in all cases different samples were used for the two methods. In addition, the columns were imaged before and after the IPTTs to evaluate the potential impacts of the tracer solution on fluid configuration and attendant interfacial area. The interfacial areas measured using IPTT are ~5 times larger than the microtomographic-measured values, which is consistent with previous work. Analysis of the image data revealed no significant impact of the tracer solution on NAPL configuration or interfacial area. Other potential sources of error were evaluated, and all were demonstrated to be insignificant. The disparity in measured interfacial areas between the two methods is attributed to the limitation of the microtomography method to characterize interfacial area associated with microscopic surface roughness due to resolution constraints.

Keywords

Multiphase; x-ray; immiscible; interfacial area; tracer test; partitioning tracer; NAPL; microtomography

1. INTRODUCTION

The interfacial area between immiscible fluids in porous media has been demonstrated to be a critical entity for improved understanding, characterization, and simulation of multifluid flow and mass transport in the subsurface. For example, it has been proposed as an additional state variable for multiphase fluid systems [e.g., Hassanizadeh and Gray, 1990;

---

[*]Corresponding Author: brusseau@email.arizona.edu.

Joekar-Niasar and Hassanizadeh, 2012], and it mediates various mass-transfer processes [e.g., *Costanza and Brusseau, 2000*; Agaoglu et al., 2015;]. The development and testing of conceptual and mathematical models incorporating fluid-fluid interface has been constrained by a lack of measurements, which in turn has limited our understanding of the role of fluid-fluid interface in flow and transport.

Two general methods have been developed to measure fluid-fluid interfacial area within 3-D porous media systems, high-resolution microtomographic imaging and interfacial partitioning tracer tests (IPTTs). In the past decade, synchrotron x-ray microtomography (XMT) has been used to characterize and quantify interfacial areas of fluid-fluid contacts within synthetic media (glass beads, plastic media), sands, and soils [Al-Raoush and Willson, 2005; Brusseau et al., 2006, 2007, 2008, 2009; Costanza-Robinson et al., 2008; Culligan et al., 2004, 2006; Ghosh and Tick, 2013; Narter and Brusseau, 2010; Prodanovic et al., 2006; Schnaar and Brusseau, 2005; 2006a; b]. Additionally, recent review papers provide examples of broader applications of high-resolution imaging [Werth et al., 2010; Blunt et al., 2013; Cnudde and Boone, 2013; Schluter et al., 2014]. Characterization of air/water and organic-liquid/water interfacial areas has also been done using various configurations of IPTTs [Anwar et al., 2000; Brusseau et al., 1997, 2006, 2007, 2008; Cho and Annable, 2005; *Costanza-Robinson and Brusseau*, 2002; Dobson et al., 2006; Jain et al., 2003; Karkare and Fort, 1996; Kim et al., 1997; 1999a,b; Narter and Brusseau, 2010; Peng and Brusseau, 2005; Saripalli et al., 1997, 1998; Schaefer et al., 2000].

The general conceptualization for fluid-fluid interface in porous media describes two components of total interfacial area, capillary interface (terminal menisci, pendular-ring/wedge menisci) and film interface. Effective application of interfacial-area measurements is predicated on a clear understanding of which interfaces are incorporated in the measurements. The results of prior studies have shown that interfacial areas measured with the IPTT method are generally larger than values measured with XMT for natural geomedia such as sands and soils [*Brusseau et al.*, 2006, 2007, 2008, 2010]. The potential cause(s) for the observed disparity in measurements have been a focus of speculation.

For example, the disparity may indicate that the two methods do not measure the same portion or fraction of total interface. This hypothesis has been proposed by Brusseau and colleagues based on several sets of experiments, including a comparative analysis employing IPTT and XMT measurements obtained for more than 10 media spanning a wide range of median grain diameters and uniformity coefficients [Brusseau et al., 2010]. Alternatively, it has been hypothesized that the observed disparity reflects erroneous measurements obtained with one of the methods, typically the IPTT method [e.g., Chen and Kibbey, 2006; Costanza-Robinson et al., 2012]. Prior investigations of this phenomenon have not been able to fully resolve the issue because either only one of the two methods was employed in the study (with the results extrapolated for comparison), or separate samples were used for the two measurement methods in studies employing both methods due to method restrictions. Thus, to date, there has been no comparative analysis conducted wherein the two measurement methods were applied to the same samples.

The objective of this investigation is to compare measurements of non-wetting/wetting interfacial area obtained contemporaneously with XMT and IPTT for the same sets of samples. This novel approach will allow a rigorous evaluation of the two opposing hypotheses that have been proposed to explain the observed disparity in measurements obtained with the IPTT and XMT methods. Additionally, this study provides an examination of all known sources of error/discrepancy between these two methods, which supports the elucidation of the cause of the disparity. The microtomographic imaging was conducted on the same packed columns that were used for the IPTTs. In addition, the columns were imaged before and after the IPTTs to evaluate potential impacts of the tracer tests on multi-fluid configuration and attendant interfacial area.

2. MATERIALS AND METHODS

2.1. Materials

The porous medium used for the experiments is a natural quartz sand (40/50 mesh Accusand, North Kato Supply) with a median grain-size diameter of 0.358 mm and a uniformity coefficient of 1.17. Reagent grade chemicals were used for all experiments (Sigma-Aldrich Co.). Trichloroethene (TCE), a common groundwater contaminant, was used as a model organic, non-wetting liquid. Iodobenzene (8% by volume) was added to the TCE to enhance image contrast between TCE and water [*Schnaar and Brusseau*, 2006b]. The addition of iodobenzene to TCE has been shown to have a negligible impact on interfacial tension, fluid configuration, and interfacial-area distribution [Schnaar and Brusseau, 2005; 2006a]. All experiments were conducted with a 5-mM $CaCl_2$ aqueous solution prepared from distilled-deionized water (Series 550, Barnstead Thermolyne Corp., Dubuque, Indiana). The interfacial partitioning and non-reactive tracers were sodium dodecylbenzene sulfonate (SDBS) (aqueous concentration of 40 mg/L) and pentafluorobenzoic acid (PFBA) (aqueous concentration of 100 mg/L), respectively.

2.2 Tracer Test Methods

The standard IPTT method for measuring interfacial area between an immiscible organic liquid and water is based on conducting tracer tests under conditions such that the non-wetting fluid exists as a trapped, immobile phase. Hence, measurements are conducted for a single non-wetting fluid saturation (i.e., at residual). The XMT experiments were therefore also conducted at a single (residual) saturation to be consistent with the IPTTs.

The IPTT experiments were conducted using Kontes Chromaflex glass chromatography columns (15 cm length and 2.5 cm inner diameter). Polypropylene frits (10 μm pore size) within the end caps promoted uniform flow and stabilized the porous media within the column, and a porous steel plate within the lower end cap was also used to promote uniform flow during imbibition. The columns were packed with sand to a consistent bulk density of 1.74 (±0.01, 95% confidence interval) under ponded water conditions, using de-aired water, to obtain water-saturated conditions.

Nonreactive tracer tests were conducted prior to establishing organic liquid saturation to characterize the hydrodynamic properties of the sand-packed columns. In addition, SDBS tracer tests were conducted to measure sorption of SDBS by the sand. The tests were conducted sequentially by introducing approximately 1–2 pore volumes of tracer solution into the column with a HPLC pump, at a pore-water velocity of ~25 cm/hr.

After the preliminary tracer tests were conducted, a residual saturation of TCE was established by first injecting approximately 2 pore-volume equivalents of pure TCE into the lower end of the vertically-oriented column with a 100 mL gas-tight syringe and a Cole Parmer 79400 Series syringe pump (pore-fluid velocity of ~15 cm/hr). Following this, an aqueous solution (TCE-saturated water) was injected into the upper end of the column using the syringe pump to displace TCE liquid and form a residual phase. A low flow rate was used for the first few pore volumes, and then increased to an equivalent maximum ~40 cm/hr pore-water velocity. The residual TCE was formed under (secondary) imbibition conditions with this procedure.

Once the residual TCE saturation was established, the column was subjected to XMT imaging. After imaging was complete, the IPTT test was conducted. Similar to the preliminary set of tracer tests, PFBA and SDBS solutions were injected sequentially by introducing approximately 2 PV of each into the column with a 100 mL gas-tight syringe using a syringe pump at a pore-water velocity of ~25 cm/hr. TCE dissolution during the experiment was minimized by preparing all SDBS and PFBA solutions with TCE-saturated water.

An UV-Vis spectrophotometer (Agilent 8453) was used to analyze the effluent samples for SDBS and PFBA. The solutions were analyzed for absorbance peaks at 223 nm and 262 nm (SDBS and PFBA peaks, respectively). Prior to analysis, the TCE in solution was removed by volatilization to prevent analytical interference.

A total of 7 sets of IPTTs were conducted, each employing a freshly packed column, except for experiments 5 and 6. These two tests were conducted with the same column pack to evaluate replicate measurements for the same column. Effluent tracer concentrations were plotted to develop breakthrough curves, which were analyzed via moment analysis to determine retardation factors (R). The total specific organic-liquid interfacial area ($a_{\mathbf{NW}}$, cm^{-1}) values were calculated with use of the following equation:

$$R=1+K_d\rho_b/\theta_w+K_i\,a_{NW}/\theta_w$$

where K_d [cm^3/g] is the solid-phase sorption coefficient, ρ_b [g/cm^3]is bulk density of the sand pack, θ_w [−] is water content, and K_i [cm] is the interfacial partition coefficient. Measurements of interfacial tension as a function of SDBS concentration were used to determine the K_i value (0.0013 cm). The contribution of SDBS retention associated with adsorption to the sand was removed from the total retardation when determining a_{NW}. Additional details regarding the execution and analysis of IPPTs can be found in Brusseau et al. [2008].

2.3. X-Ray Microtomography

XMT imaging was conducted for all 7 IPTT experiments at the Environmental Molecular Sciences Laboratory (EMSL). Instrumentation and methods for the imaging are described in Carroll et al. [2015]. The entire column length was scanned at one time, with a resolution of ~22 μm. Segmentation and phase quantification was conducted using the Blob3D software [*Ketcham*, 2005], which employs a global-thresholding approach, following previously described methods [Schnaar and Brusseau, 2005; 2006a]. These methods have been used to produce accurate *in situ* characterization of non-wetting fluid volumes, surface areas, and fluid-fluid interfacial areas [*e.g., Brusseau et al.*, 2008; Narter and Brusseau, 2010; Schnaar and Brusseau, 2005], which are the measurements of interest for the present study.

The volume of all the voxels contained within each individual blob of contiguous organic-liquid voxels was determined, and the sum of individual blob volumes was used to calculate the total organic-liquid volume. Isosurface smoothing was used within Blob3D to minimize pixilation of smooth surfaces attributed to the finite imaging resolution and data binarization associated with thresholding. The isosurface area between TCE and water was determined, representing the absolute total organic-liquid/water interfacial area. The absolute interfacial area was divided by the total volume of the porous medium to calculate the $a_{\mathbf{NW}}$ values. The solid specific surface area was also calculated from direct imaging and processing of the solid phase. This value was compared to the geometric specific solid surface area, which was calculated as (6(1-n))/d with n as the porosity and d as the median grain diameter. This equation is based on algebraic simplification of the quotient of surface area and volume for a smooth sphere.

3. RESULTS AND DISCUSSION

3.1 IPTT Results

Prior to introducing TCE into each column, tests were conducted with both tracers to characterize the hydrodynamics of each column and SDBS sorption by the sand. The breakthrough curves for PFBA and SDBS were symmetrical, indicating minimal dispersion (data not shown). The retardation factors for PFBA were ~1, indicating its transport was not retarded and that it served as an effective non-reactive tracer. Very slight retardation was observed for SDBS, indicating a small degree of sorption. The mean sorption coefficient for SDBS was 0.019 mL/g (±0.016), which is similar to results reported for the same sand in previous work [Brusseau et al., 2008].

Following formation of residual TCE saturation, tracer tests were again conducted for each column. Retardation factors less than 1 ($\bar{R}$ = 0.77 ±0.04) were obtained for PFBA, as expected, reflecting the presence of TCE liquid in some regions of the pore space. The R values are consistent with the TCE saturations ($\bar{S}_n$ = 0.23 ±0.07). Measureable retardation was observed for SDBS, with $\bar{R}$ = 1.5 (±0.1), for all experiments. Analysis of the IPTT data yielded a mean organic-liquid/water specific interfacial area of 75 (±20) cm^{-1}.

3.2 XMT Results

Images obtained using XMT showed that water, sand, and TCE could be easily differentiated (Figure 1). TCE was well distributed radially throughout the columns, and there appeared to be no preferential accumulation along the column walls. Organic-liquid blobs ranged in size from small, spherical singlets to large ganglia greater than 4 mm in length, which is consistent with previous work [Al-Raoush, 2009; Al-Raoush and Willson, 2005; Ghosh and Tick, 2013; Schnaar and Brusseau, 2005].

The mean porosity determined from the image data (quotient of fluid volume and imaged volume) for all 6 columns is 0.32 (±0.02), which is statistically identical to the porosity determined from gravimetric analysis (0.34 ±0.01). The specific solid surface area calculated from direct imaging of the solids is 95 (±4) cm^{-1}. This result is similar to the geometric solid surface area of 110 (±8) cm^{-1}. These results indicate that the XMT image acquisition and processing methods provided robust results. The mean organic-liquid/water specific interfacial area measured from the XMT data is 14.7 (±2) cm^{-1}.

3.3 Comparison of IPTT and XMT Results

The mean interfacial area measured using the IPTT method (75 ±20 cm^{-1}) is approximately 5 times larger than the mean measured using XMT (14.7 ±2 cm^{-1}). This result is consistent with prior studies comparing these two methods for natural media [Br*usseau et al.*, 2006, 2007, 2008]. Brusseau et al. *[2008]* comprehensively examined a number of factors that could potentially cause the observed discrepancy between the IPTT and XMT values, including: errors in the IPTT method (e.g., impact of the surfactant tracer on fluid distribution and configuration), IPTT performance constraints (e.g., hydraulic accessibility of interfaces; mass-transfer constraints), uncertainty in quantification of tracer sorption by the solid phase, systematic error in the XMT method, and characterization of different samples. This last factor was eliminated in the current study by imaging the same columns that were used for the IPTTs.

One recurring concern associated with the use of surfactant tracers for the IPTT method is the potential impact of the tracer solution on the distribution and configuration of the fluids, including mobilization of the organic liquid and drainage of the wetting phase due to changes in interfacial tension, and attendant alterations of interfacial area. The columns were imaged before and after the IPTT to specifically examine this issue. No measurable impacts were observed, as illustrated by the XMT results obtained for experiments 5 and 6. Multiple IPTTs were conducted sequentially for the same column with these two experiments, and there was no statistically significant difference in the XMT-measured a_{NW} values (1% difference). This result demonstrates that multiple additions of SDBS solution had no impact on measurement of a_{NW}. This result is consistent with those of Brusseau et al. *[2008]*, who also examined the potential impact of SDBS solutions on the distribution and configuration of fluids by imaging columns containing organic liquid at residual saturations before and after introduction of SDBS solution. They reported no significant change in the distribution and configuration of fluids. Furthermore, the difference between the specific interfacial areas measured before and after introduction of the SDBS solution was less than 5%, which is within measurement error. In total, these results indicate that the injection of the surfactant tracer solution had negligible impact on the configuration of the immiscible fluid phases, and thus did not create artifacts for the measurement of interfacial areas.

Another concern with the use of surfactant tracers is possible alteration of solid-surface wettability due to surfactant adsorption. This wettability alteration could, in turn, influence fluid configuration and/or distribution, and hence interfacial area. The potential impact of this phenomenon is anticipated to be small given that sorption of SDBS by the sand is very low. In addition, the similarity in a_{NW} values obtained for experiment 5 and 6, in conjunction with the imaging results discussed in the prior paragraph, indicates that there was no measurable impact of wettability alteration of the porous medium.

An additional concern with the use of the IPTT method is the potential for hydraulic and/or mass-transfer constraints limiting the accessibility of the tracer to all available fluid-fluid interface. If accessibility constraints were influencing the performance of the IPTT, the resultant impact would cause the measured interfacial areas to be smaller than their true values. Given that the IPTT-measured values are larger than the XMT-measured values, potential accessibility limitations associated with the IPTT method cannot account for the observed discrepancy.

Uncertainty in the quantification of solid-phase sorption of the SDBS is another factor that can impact the magnitude of the specific interfacial area determined using the IPTT method. Underestimation of the sorption coefficient can lead to artificially high interfacial areas while overestimation will lead to the opposite. In this study, a mean K_d value of 0.019 (mL/g) was measured for SDBS sorption. In order to assess if sorption uncertainty could be responsible for the difference between the XMT and IPTT methods, the upper-range (99% confidence interval) K_d value of 0.04 (mL/g) was also used in the determination of interfacial area for the IPTTs. This resulted in a mean interfacial area of 48 ± 20 cm^{-1}. This value and the calculated confidence interval remain significantly greater than the XMT-measured values (14.7 ± 2 cm^{-1}).

As noted above, the XMT image acquisition and processing methods appear to be robust based on comparison of XMT-measured porosity and specific solid surface area to independently obtained values. In particular, the similarity of the values indicates that XMT characterized the entire pore network. This is consistent with the imaging resolution (~20 μm) and the pore-size distribution of the sand, for which 95% of the pores have a nominal diameter of 100 μm or larger (data not shown).

Based on the above analysis, both methods are deemed to have produced robust data, with no apparent significant sources of error or artifacts serving as the cause of the disparity in measured interfacial areas. As noted above, different magnitudes of interfacial area have been measured with XMT and IPTT for the same natural geomedia in prior studies. Conversely, identical values were obtained when both methods were applied to a glass-bead medium that had smooth surfaces [Narter and Brusseau, 2010]. This latter result clearly demonstrates that the two methods can produce comparable values under certain conditions. Furthermore, given that the IPTT method is more often considered to be the method more prone to potential error, this result demonstrates that the IPTT method can produce robust values as validated by imaging-based measurement.

Previously, it has been hypothesized that thin-film interfacial area associated with surface roughness is a primary cause of the observed disparity in interfacial areas obtained with the XMT and IPTT methods [B*russeau et al.*, 2007, 2008, 2010] and for the observation that IPTT-measured interfacial areas are greater than geometric-based solid surface areas [Kim et al., 1997, 1999a,b; Saripalli et al., 1997]. In the present study, the XMT and geometric specific solid surface areas, 95 and 110 cm^{-1}, respectively, are both more than 10 times smaller than the specific solid surface area measured with the N_2/Brunauer, Emmett, and Teller (N_2/BET) method (1363 ±90 cm^{-1}). In addition, the estimated maximum specific interfacial area determined from the IPTTs (331 cm^{-1}, determined as $A_{max} = a_{NW}/S_n$), is significantly larger than the XMT-measured and geometric-estimated specific solid surface areas. These results are consistent with the cited previous work. It is known that the BET method provides a measure of surface area associated with microscopic surface roughness, which is not characterized by XMT due to resolution limitations. Given that potential errors and artifacts associated with XMT and IPTT measurements were eliminated from consideration, it is concluded that unresolved surface roughness was responsible for the majority of the observed discrepancy between the XMT- and IPTT-measured a_{NW} values.

The results of this study indicate that XMT and IPTT are both accurate methods of measuring fluid-fluid interfacial area, but that they characterize different components of the interfacial domain. XMT provides robust measurements of capillary-associated interfacial area, which are critical for simulation of multiphase flow. The IPTT method provides measures of “total” interfacial area, including that associated with thin wetting-fluid films, useful for characterizing mass-transfer processes.

Acknowledgments

This work was supported by the NIEHS Superfund Basic Research Program (P42 ES04940). Imaging was conducted with the support of user proposals at the Environmental Molecular Sciences Laboratory (EMSL), which is a user facility sponsored by the DOE Office of Biological and Environmental Research (Proposal # 44728). We thank Matthew Narter (University of Arizona) and Dr. Tomas Varga (EMSL) for their assistance. We also thank the reviewers and editors for their constructive comments. Raw data used in this work are available upon request.

References

Agaoglu B, Copty NK, Scheytt T, Hinkelmann R. Interphase mass transfer between fluids in subsurface formations: A review. Advances in Water Resources. 2015; 79:162–194.

Al-Raoush RI. Impact of Wettability on Pore-Scale Characteristics of Residual Nonaqueous Phase Liquids. Environmental Science & Technology. 2009; 43(13):4796–4801. [PubMed: 19673267]

Al-Raoush RI, Willson CS. A pore-scale investigation of a multiphase porous media system. Journal of Contaminant Hydrology. 2005; 77(1–2):67–89. [PubMed: 15722173]

Anwar AHMF, Bettahar M, Matsubayashi U. A method for determining air-water interfacial area in variably saturated porous media. Journal of Contaminant Hydrology. 2000; 43(2):129–146.

Brusseau ML, Popovicova J, Silva JAK. Characterizing gas-water interfacial and bulk water partitioning for gas phase transport of organic contaminants in unsaturated porous media. Environmental Science & Technology. 1997; 31(6):1645–1649.

Brusseau ML, Peng S, Schnaar G, Costanza-Robinson MS. Relationships among air-water interfacial area, capillary pressure, and water saturation for a sandy porous medium. Water Resources Research. 2006; 42(3)

Brusseau ML, Peng S, Schnaar G, Murao A. Measuring air–water interfacial areas with x-ray microtomography and interfacial partitioning tracer tests. Environmental Science & Technology. 2007; 41(6):1956–1961. [PubMed: 17410790]

Brusseau ML, Janousek H, Murao A, Schnaar G. Synchrotron X-ray microtomography and interfacial partitioning tracer test measurements of NAPL-water interfacial areas. Water Resources Research. 2008; 44(1)

Brusseau ML, Narter M, Schnaar G, Marble J. Measurement and estimation of organic-liquid/water interfacial areas for several natural porous media. Environmental Science & Technology. 2009; 43(10):3619–3625. [PubMed: 19544863]

Brusseau ML, Narter N, Janousek H. Interfacial partitioning tracer test measurements of organic-liquid/water interfacial areas: application to soils and the influence of surface roughness. Environ Sci Technol. 2010; 44:7596–7600. [PubMed: 20825178]

Carroll KC, McDonald K, Marble J, Russo AE, Brusseau ML. The impact of transitions between two-fluid and three-fluid phases on fluid configuration and fluid-fluid interfacial area in porous media. Water Resour Res. 2015; 51:7189–7201. [PubMed: 27350722]

Chen L, Kibbey TCG. Measurement of air_water interfacial area for multiple hysteretic drainage curves in an unsaturated fine sand. Langmuir. 2006; 22(16):6874–6880. [PubMed: 16863233]

Cho JY, Annable MD. Characterization of pore scale NAPL morphology in homogeneous sands as a function of grain size and NAPL dissolution. Chemosphere. 2005; 61(7):899–908. [PubMed: 15950262]

Costanza MS, Brusseau ML. Contaminant vapor adsorption at the gas-water interface in soils. Environmental Science & Technology. 2000; 34(1):1–11.

Costanza-Robinson MS, Brusseau ML. Air-water interfacial areas in unsaturated soils: Evaluation of interfacial domains. Water Resources Research. 2002; 38(10)

Costanza-Robinson MS, Harrold KH, Lieb-Lappen RM. X-ray microtomography determination of air-water interfacial area-water saturation relationships in sandy porous media. Environmental Science & Technology. 2008; 42(8):2949–2956. [PubMed: 18497149]

Costanza-Robinson, MS., Zheng, Z., Henry, EJ., Estabrook Benjamin, D., Littlefield, MH. Implications of surfactant-induced flow for miscible-displacement estimation of air_water interfacial areas in unsaturated porous media. Environ Sci Technol. 2012. http://dx.doi.org/10.1021/es303003v

Culligan KA, Wildenschild D, Christensen BSB, Gray WG, Rivers ML. Pore-scale characteristics of multiphase flow in porous media: A comparison of air-water and oil-water experiments. Advances in Water Resources. 2006; 29(2):227–238.

Culligan KA, Wildenschild D, Christensen BS, Gray WG, Rivers ML, Tompson AFB. Interfacial area measurements for unsaturated flow through a porous medium. Water Resources Research. 2004; 40(12)

Dobson R, Schroth MH, Oostrom M, Zeyer J. Determination of NAPL-water interfacial areas in well-characterized porous media. Environmental Science & Technology. 2006; 40(3):815–822. [PubMed: 16509323]

Ghosh J, Tick GR. A pore scale investigation of crude oil distribution and removal from homogeneous porous media during surfactant-induced remediation. Journal of Contaminant Hydrology. 2013; 155:20–30. [PubMed: 24113292]

Hassanizadeh SM, Gray WG. Mechanics and thermodynamics of multiphase flow in porous media including interphase boundaries. Advances in water resources. 1990; 13(4):169–186.

Jain V, Bryant S, Sharma M. Influence of wettability and saturation on liquid-liquid interfacial area in porous media. Environmental Science & Technology. 2003; 37(3):584–591. [PubMed: 12630476]

Joekar-Niasar V, Hassanizadeh SM. Analysis of Fundamentals of Two-Phase Flow in Porous Media Using Dynamic Pore-Network Models: A Review. Critical Reviews in Environmental Science and Technology. 2012; 42(18):1895–1976.

Ketcham RA. Computational methods for quantitative analysis of three-dimensional features in geological specimens. Geosphere. 2005; 1:32–41.

Karkare MV, Fort T. Determination of the air-water interfacial area in wet “unsaturated” porous media. Langmuir. 1996; 12(8):2041–2044.

Kim H, Rao PSC, Annable MD. Determination of effective air-water interfacial area in partially saturated porous media using surfactant adsorption. Water Resources Research. 1997; 33(12): 2705–2711.

Kim H, Rao PSC, Annable MD. Gaseous tracer technique for estimating air-water interfacial areas and interface mobility. Soil Science Society of America Journal. 1999a; 63(6):1554–1560.

Kim H, Rao PSC, Annable MD. Consistency of the interfacial tracer technique: experimental evaluation. Journal of Contaminant Hydrology. 1999b; 40(1):79–94.

Narter M, Brusseau ML. Comparison of interfacial partitioning tracer test and high-resolution microtomography measurements of fluid-fluid interfacial areas for an ideal porous medium. Water Resources Research. 2010; 46(8):W08602.

Peng S, Brusseau ML. Impact of soil texture on air-water interfacial areas in unsaturated sandy porous media. Water Resources Research. 2005; 41(3)

Prodanovic M, Lindquist WB, Seright RS. Porous structure and fluid partitioning in polyethylene cores from 3D X-ray microtomographic imaging. Journal of Colloid and Interface Science. 2006; 298(1):282–297. [PubMed: 16364351]

Saripalli KP, Rao PSC, Annable MD. Determination of specific NAPL-water interfacial areas of residual NAPLs in porous media using the interfacial tracers technique. Journal of Contaminant Hydrology. 1998; 30(3–4):375–391.

Saripalli KP, Kim H, Rao PSC, Annable MD. Measurement of specific fluid - Fluid interfacial areas of immiscible fluids in porous media. Environmental Science & Technology. 1997; 31(3):932–936.

Schaefer CE, DiCarlo DA, Blunt MJ. Determination of water-oil interfacial area during 3-phase gravity drainage in porous media. Journal of Colloid and Interface Science. 2000; 221(2):308–312. [PubMed: 10631035]

Schluter S, Sheppard A, Brown K, Wildenschild D. Image processing of multiphase images obtained via X- ray microtomography: A review, Water Resources Research. 2014; 50(4):3615–3639.

Schnaar G, Brusseau ML. Pore-scale characterization of organic immiscible-liquid morphology in natural porous media using synchrotron X-ray microtomography. Environmental Science & Technology. 2005; 39(21):8403–8410. [PubMed: 16294880]

Schnaar G, Brusseau ML. Characterizing pore-scale dissolution of organic immiscible liquid in natural porous media using synchrotron X-ray microtomography. Environmental Science & Technology. 2006a; 40(21):6622–6629. [PubMed: 17144287]

Schnaar G, Brusseau ML. Characterizing pore-scale configuration of organic immiscible liquid in multiphase systems with synchrotron X-ray microtomography. Vadose Zone Journal. 2006b; 5(2): 641–648.

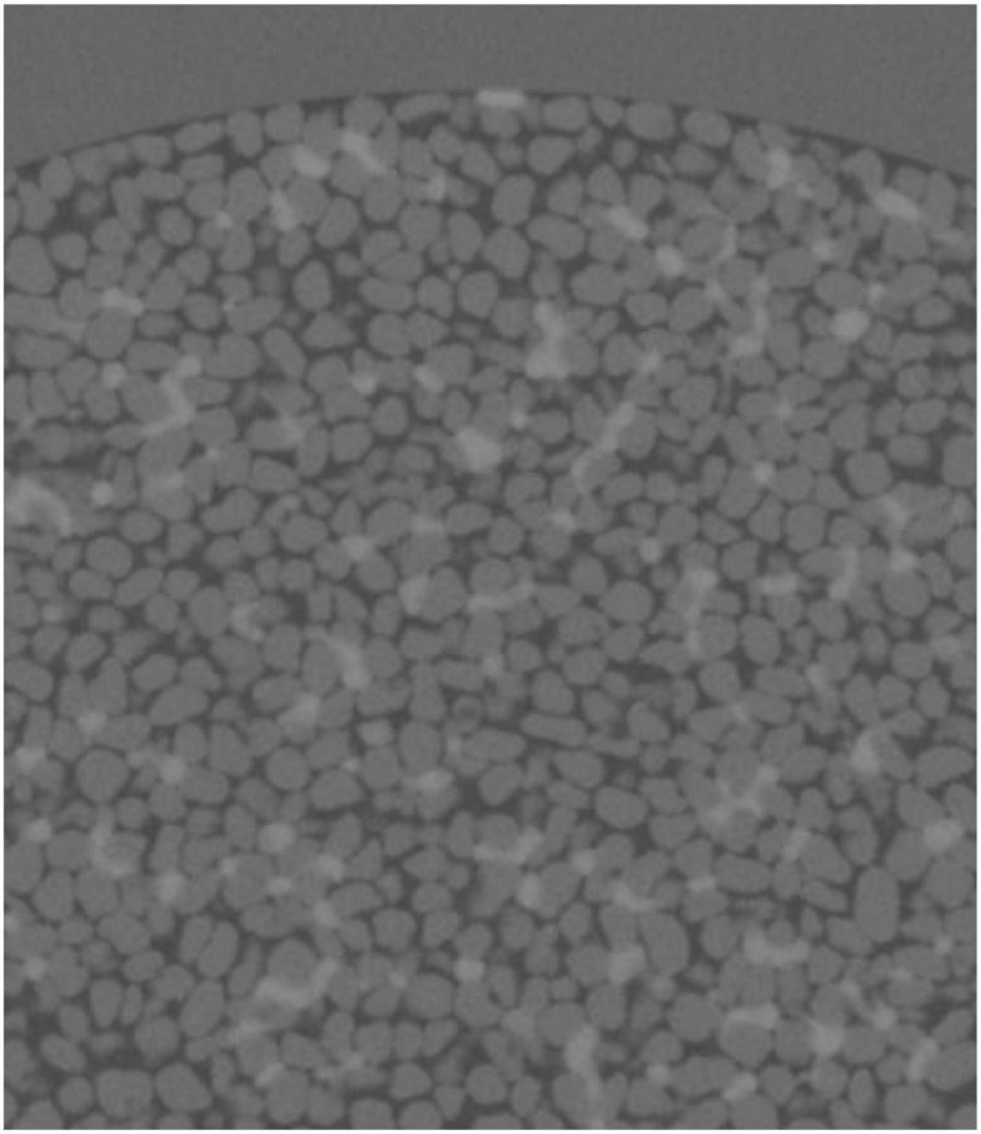

Figure 1.

Original gray-scale image obtained from XMT. The section of the column cross-section shown is approximately 8 x 8 mm. The light gray objects are the sand grains, the dark gray is the water, and the white is the TCE blobs. A section of the column wall is present in the top of the image.